Constrained Moment Tensors: Source Models and Case Studies

Jan Šílený

1 Introduction—The Moment Tensor

In recent decades, the earthquake mechanism, regardless of scale, has commonly come to be described by the moment tensor (MT). The MT has been used when inverting local but, especially, teleseismic (Global CMT project: Dziewonski et al. 1981; Ekstrom et al. 2012; USGS: Sipkin 1982; Sipkin and Zirbes 2004; ERI: Kawakatsu 1995) and regional (e.g., Dreger and Helmberger 1993; Ritsema and Lay 1993; Nábělek and Xia 1995; Braunmiller et al. 2002; Pondrelli et al. 2002; Stich et al. 2003; Kubo et al. 2002) data. For local data, here, I cite events occurring within earthquake swarms (Jakobsdóttir et al. 2008; Horálek and Fischer 2008).

The unconstrained MT is the most comprehensive description of shear and non-shear sources and is the body force equivalent of a rupture (i.e. it consists of a system of forces, in fact, force couples) that generates the same wave field in a continuous medium as an actual rupture. In this way, it is not a physical source but substitutes for real processes occurring within the focus. As a system of body forces, the MT is not a priori convenient for offering a simple perception of an earthquake focus. Therefore, for the sake of interpretation, the MT is generally decomposed into simple sources. The method of decomposition is not unique. The most commonly and widely used procedure is one that splits the general MT into isotropic and deviatoric portions (unique), and then splits the deviatoric portion into a double couple (DC) and a compensated linear vector dipole (CLVD) with a common major tension or pressure axis (ambiguous). The somewhat painful procedure of searching for a reasonable decomposition amongst a theoretically infinite number of processes is described in Julian et al. (1998). The MT captures general combinations of dipoles and, as such, is able to approach a wide class of mechanisms that can occur within an earthquake source. An important advantage of the MT description is a linear relationship between

J. Šílený (✉)
Institute of Geophysics, Czech Academy of Sciences, Prague, Czech Republic
e-mail: jsi@ig.cas.cz

S. D’Amico (ed.), *Moment Tensor Solutions*, Springer Natural Hazards,
https://doi.org/10.1007/978-3-319-77359-9_9

source parameters and seismic observations (through the response of a medium, Green's function) that implies linearity for the inversion task. As such, the MT allows fast and unique retrieval of the six independent parameters—M_{11}, M_{12}, M_{13}, M_{22}, M_{23}, and M_{33}—without the need to specify an initial guess.

The MT is not only the most general description of a mechanism relevant to an earthquake source. In general, it is also relevant to the fracturing of a solid body, including all of the modes of fracturing recognized within fracture mechanics and their combinations. However, the MT also includes mechanisms that do not generally represent realistic physical sources because it does not describe the rupture itself but rather body force equivalents of actual rupturing. As such, the MT is needlessly general. In addition to rupture mode I (tensile fracturing), rupture modes II and III (plane and anti-plane shear slip), combinations of force systems that do not correspond to a physically feasible rupturing are also present. Therefore, for the simple rupturing expected within the foci of tectonic earthquakes, the MT is unnecessarily complex, leading to more parameters than those relevant to simple rupture models.

2 Constraining the Moment Tensor

From the viewpoint of solving the inverse problem of earthquake mechanism retrieval from seismic data, the tax of an advantage of linearity for the inverse task employing the MT as the source mechanism description is potentially small robustness in cases where the inverse problem is not well-posed (e.g. if the data are sparse or of low quality, or if the hypocenter localization or velocity/attenuation model of the medium are uncertain (e.g., Šílený et al. 1992; Dahm et al 2000; Stierle et al. 2014)). Therefore, in practice, it is advantageous to reduce generality within the MT (i.e., to decrease the number of parameters within the source mechanism model from six, for the MT, to five or four). The endpoint of this sequence is a DC that is described by three angles that depict the orientation of the corresponding shear slip and its size, capturing its scalar moment.

A widely used constraint is the deviatoric MT, where the MT trace preserves a zero value:

$$M_{11} + M_{22} + M_{33} = 0 \quad (1)$$

As a default, the deviatoric MT is applied within Global and Regional CMT procedures in order to simplify the MT to make an inversion more stable and to approach the shear slip as the foreseen mechanism for tectonic earthquakes. The result is a zero volume change within the focus. In spite of this, the constraint does not imply that the mechanism described is a desirable shear slip. The deviatoric MT contains both a double-couple (DC) (the equivalent of a pure shear slip along a plane fault embedded within an isotropic medium), as well as a compensated linear-vector dipole (CLVD). The CLVD is an artifact of the decomposition and, by itself, lacks clear physical interpretation. From this perspective, the deviatoric constraint is not ideal. Although the deviatoric constraint is widely used, its only advantage is that it maintains the linearity of the inverse task for unconstrained MT retrieval. Much of the use of Global CMT catalogs, as well as regional CMT catalogs, concern utilization of the DC portion of the CMT solution—its association to faults within the area under study, interpretation in terms of regional and local tectonics, etc. However, a DC obtained in this way, a traditional "best DC" (i.e. a component isolated from the MT obtained as a solution to the inverse problem), is not equal to a directly retrieved DC. Henry et al. (2002) demonstrated that the DC, decomposed from the MT, can be biased due to inaccurate velocity models and that this type of DC is only reliable when the non-DC component of the MT solution is small.

For completeness, the purely isotropic source itself, the complement to the deviatoric MT, should also be considered to be a constrained MT. The importance of this source model rests in the fact that explosions are processes that basically approach isotropic expansion. However, this may be modified by inhomogeneity and/or the anisotropy of the medium of the focal zone, the latter being caused by both intrinsic properties of the geologic material or by the state of pre-stress, as demonstrated by Vavryčuk and Kim (2014). Also, in industry, due to the technology of blasting, blasts may be far from isotropic expansion, especially blasts within a series of delayed shocks. Such a series may be perceived as a single event depending on the frequency window of the observation and possesses radiation directivity related to the geometry of the blast series.

The deviatoric constraint is a formal approach for reducing the number of parameters describing the source mechanism, as originated by a mathematical concept. A different approach is to constrain the MT by accepting some idea regarding the physics of rupturing during earthquake activity within the focus. An obvious procedure is assuming a fault within the focus and the earthquake process as a sudden slip on the fault. This idea leads to an equation relating the MT to fault and slip vectors (within an isotropic medium; Aki and Richards 2002, Eq. 3.21), as follows:

$$M_{ij} = \lambda n_k u_k \delta_{ij} + \mu \left(n_i u_j + n_j u_i \right) \tag{2}$$

where **n** and **u** are the fault normal and slip vector, respectively; and λ and μ are the Lamé constants. Although the setup of this source model is fairly generic and capable of describing many situations that researchers believe may occur within the earthquake focus, it is less general than the full MT. For example, it cannot describe a purely isotropic source (1).

Both implicit or explicit, the constraint (2) is the basis of many models for a seismic source. The former group consists of models intuitively designed to describe natural or man-made setups that are related to the occurrence of seismicity and are not formally treated using mathematics. For example, Hasegawa et al. (1989) suggested a series of models designed to describe seismoactive phenomena occurring in mines: (i) a single force for a cavity collapse, (ii) a vertical compressive single couple for a pillar burst, (iii) a vertical tensile crack for a cavity roof break, and (iv) combinations of implosion within a dip slip for a stope and cavity closure (Fig. 1, the b/w background). To be specific, model (i) is outside the framework of the moment

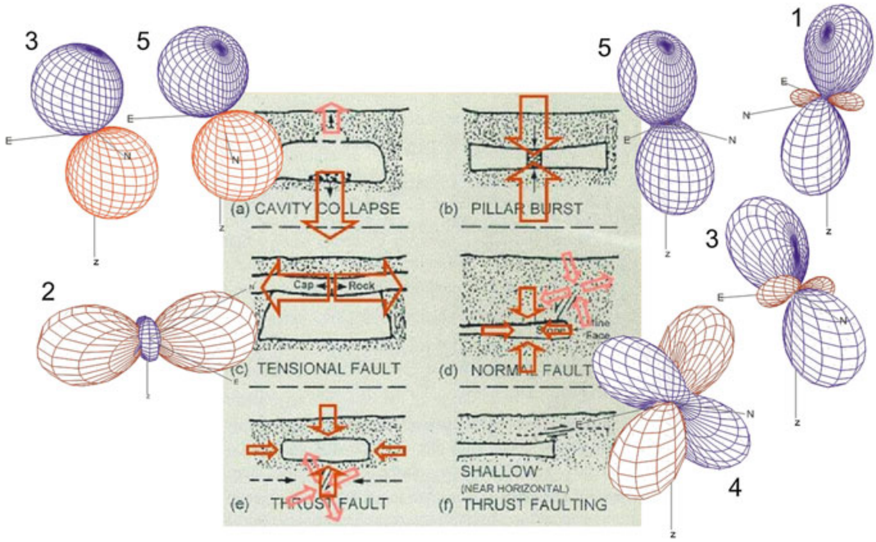

Fig. 1 Models (**a**–**f**) for seismoactive events occurring in mines by Hasegawa et al. (1989) (black/white background) and their body-force equivalents (red and rose arrows). 3D views of the P-radiation pattern for five Ridgeway mine events obtained using the inversion of P and S amplitudes are found as wireframe diagrams on the margin

tensor concept because a single force is applied as the equivalent for the break of the cavity roof (the MT consists of couples of forces). Additionally, for a more exact consideration, the equivalent for cavity roof collapse is a couple of single forces related to the detachment of rock from the roof and to its subsequent fall to the floor (Malovichko 2005). Below, in Fig. 1, body-force equivalents corresponding to individual physical phenomena (a–d) are marked using red/rose arrows.

Šílený and Milev (2008) applied the MT and single force models when inverting direct P and S amplitudes for the five seismic events recorded within the Driefontein gold mine in South Africa with the aim of interpreting their mechanisms in terms of the Hasegawa models. For two events (3 and 5), both a downward single force and nearly a vertical compressional single couple equally fit the data (i.e. a cavity collapse and a pilar burst were both plausible). A pillar burst may have also occurred for event 1, while event 2, with a nearly extensional single couple, may have corresponded to a break of the cavity roof. A comparison with the mine map documented a coincidence for the hypocentra within the mine works. Thus, the Hasegawa models seem to have been useful.

Explicitly, models related to (2) or to combinations of these models have appeared in numerous papers. Combinations are largely comprised of a traditional model for an earthquake mechanism, a pure shear slip along a fault within body-force equivalents corresponding to a DC, and an additional component designed to simulate a particular feature of an event to be investigated. As early as the 1980s, Teisseyre (1980) proposed several configurations for a shear-slip (with opening or closing tensile cracks at the

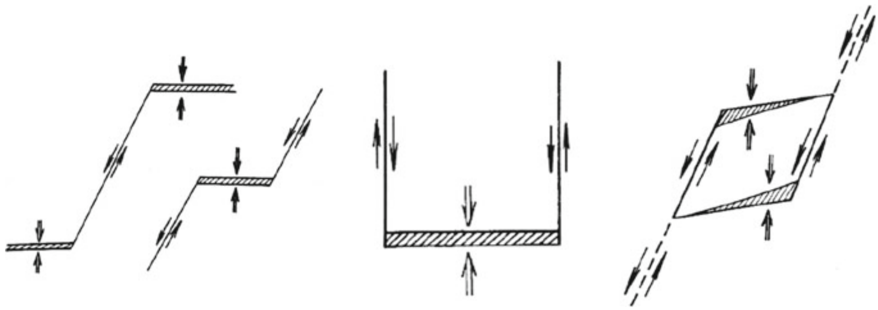

Fig. 2 Models of rockburst foci by Teisseyre (1980). From left to right: a simple shearing, shearing with compression, a complex opposite shearing, and a closed pattern for the rockburst process

tips of the fault) in order to simulate complex fracturing in either the extensional or compressional regime, the latter intended to describe a rockburst focus (Fig. 2). However, Teisseyre (1980) did not solve for the angle of the tensile crack with respect to fault direction, so the model remained conceptual.

The concept of Teisseyre (1980) was employed by Rudajev and Šílený (1985) and Šílený (1989) for inverting local seismic data related to mining tremors occurring within Kladno and Ostrava, Czechoslovakia, coal mines. Rudajev and Šílený (1985) embedded a model of a shear fault and a closing crack running perpendicular from its tip. In Šílený (1989), to avoid doubts regarding the precise angle of the tensile crack, the shear fault was complemented by an isotropic implosion. The combination of a shear fault with a tensile crack leaving the fault tip at various angles was studied by Julian et al. (1998) who investigated the radiation of such a source independent of the geometry of the fault versus the tensile crack and the direction of the opening.

A special case of geometry amongst the Julian et al. (1998) superpositions of a shear fault with a tensile crack is the geometry that occurs when the tensile crack formally coincides with a shear fault and opens perpendicularly to the fault. At the same time, this geometry is the genuine source described by (2). Previously described models were combinations of two or more sources compatible with (2). The one just described can be interpreted as a shear fault that simultaneously opens (or closes) with shear slipping. Although differently named by various authors, here, I refer to it as a shear-tensile crack (STC).

3 Shear-Tensile Crack (STC)

The concept of the shear slip and a simultaneous opening of the same fault originated in Dufumier and Rivera (1997), afterward appeared in Minson et al. (2007), and was revisited by Vavryčuk (2001, 2011). A big advantage in comparison to the MT is the fact that STC is a physically based concept for the source mechanism; simply, a

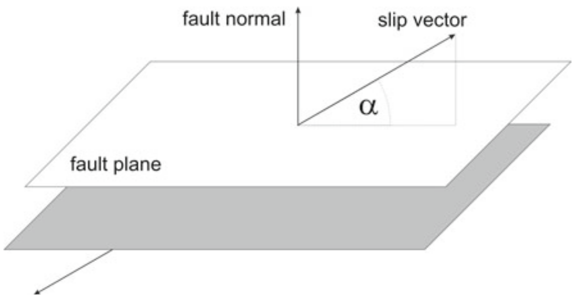

Fig. 3 The STC source model: a combination of shear-slip and tensile crack represented by the slip vector off the fault plane with the slope angle α (α = 0° is a pure shear slip and α = 90° is a tensile crack)

slip along a fault that may open or close at the same time (i.e. directly describing the seismoactive process in terms of the rupture occurring within the focus), Fig. 3.

At the same time, a source model representing a constrained MT is described by five parameters: (i) the dip of the fault, (ii) the strike of the fault, (iii) the rake angle specifying the shear component of the slip, (iv) angle, α, referred to as the slope, representing the off-plane component of the slip vector, and (v) the magnitude. The number of parameters is the same as that for the deviatoric MT. Contrarily, however, the model also has the capability of describing a change in volume within the focus. In fact, it is the simplest source model for incorporating a shear slip and a volume change. In this way, it combines a desirable amount of generality with maximum possible simplicity, ensuring robustness for the inverse task (Šílený 2009; Pesicek et al. 2012).

Despite the constraint in comparison to the full MT, the STC is a source model that is amazingly flexible with a varying slope angle, the endpoints being a traditional shear-slip (with a DC as its body force equivalent) and a tensile crack, Fig. 4. Thus, the properties of radiation change from the well-known quadrant pattern of the DC to the all-positive (or, alternatively, negative in the option of an implosion) onset of a P-wave. A similar feature, a change from a four lobbed pattern to a bimodal appearance, is also seen in the radiation of S waves. Illustrative behavior can be observed at the source planes (source lines within the projection onto the horizontal plane). Source planes within the STC include the plane of the fault that tangentially slips and the plane perpendicular to the slip vector (Vavryčuk 2001, 2011). For the pure shear-slip, the planes coincide with the traditional nodal planes of the fault-plane solution. With an increasing slope, they deviate from their originally perpendicular configuration. For the tensile crack, they merge into a single plane, namely, the plane of the crack.

In the design of their model, Dufumier and Rivera (1997) were motivated by thoughts regarding the relationship of a full moment tensor applied to tectonic earthquakes and rheological constraints, which may not always be realistic. Their solution was the proposal of an extended physical model that included tectonic and non-tectonic volumetric variations. Minson et al. (2007) essentially used the same model but referred to it as the CDC—the "crack plus double couple". They reminded readers that the model was used for geodetic inversions of seismic sources by Okada (1985)

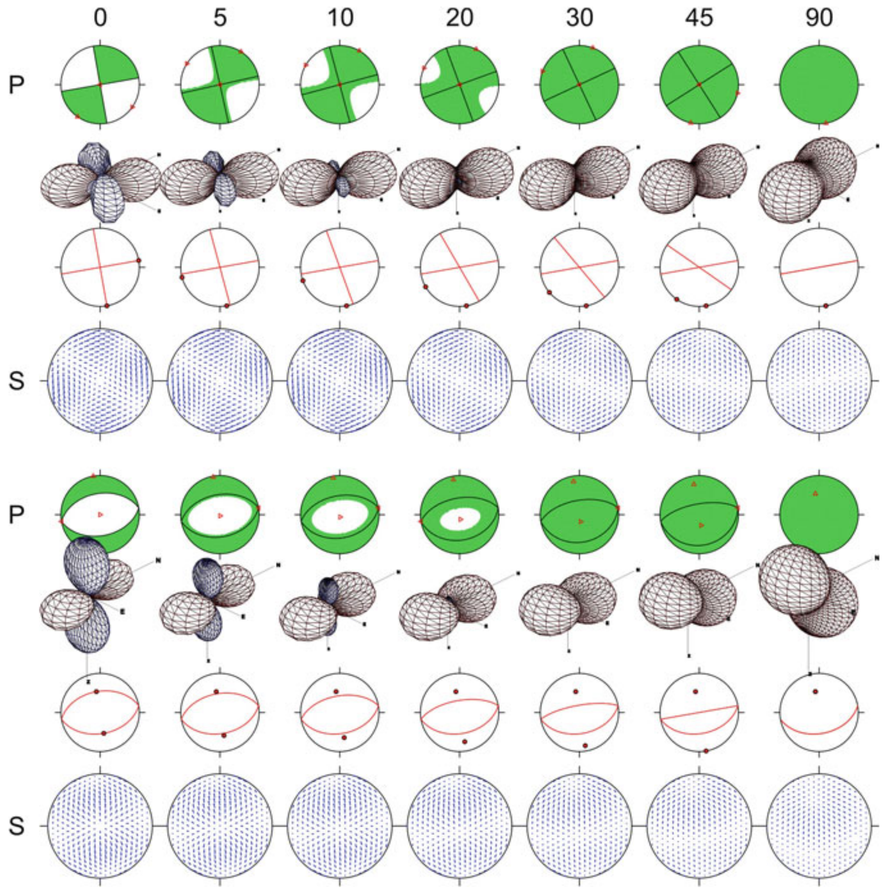

Fig. 4 Plots of the radiation pattern of P and S waves of the shear-tensile crack (STC) source dependent of the acquiring slope angle of 0, 5, 10, 20, 30, 45, and 90°. The upper half of the figure displays the vertical strike-slip mechanism. The lower half displays the dip-slip inclined 45° from the vertical. Row 1: traditional fault-plane solution plots (nodal lines, zones of compression for P-waves in green; principal axes, red triangles (T-axis, triangle up; P-axis, triangle right; N-axis, triangle left). Row 2: wireframe diagrams of P-radiation in 3-D (compressions, red; dilations, blue). Row 3: source lines (red lines) and poles of the source planes (red circles). Row 4: the S-radiation pattern (projection of polarization vectors of S-waves). In rows 1, 2, and 4, equal area projections of the lower hemisphere are used

and they applied it in order to interpret data from a volcanic earthquake swarm in Japan that had obvious volume changes within the focus. Features of the model were investigated, in detail, from the point of view of the theory by Vavryčuk (2001, 2011). Vavryčuk (2001, 2011) referred to events with both shear slip and tensile components as "tensile earthquakes". He derived various useful formulas for the decomposition of the equivalent moment tensor and the source tensor for the slope angle, and introduced source planes, the fault plane and the plane perpendicular to the slip vector, as analogues to nodal planes known from the DC.

To retrieve a reliable earthquake mechanism, data of sufficient quality from directions surroundings the hypocenter should be available. Such a condition is required for any seismic event. As far as small earthquakes are concerned, a generally low signal to noise ratio and limited data due to sparse observations are additional obstacles. Pesicek et al. (2012) and Šílený et al. (2014) recently investigated this topic in detail by performing a series of synthetic tests that explored: (i) various types of station distributions from very good to very poor, (ii) inaccurate locations for hypocenters, (iii) improper modeling for velocities, (iv) the noise contamination of data, and (v) the compatibility of results obtained using different techniques. These authors demonstrated that: (1) the number of stations and the regularity of their distribution are crucially important for the retrieval of both the orientation of the source mechanism and the DC versus non-DC content, (2) noise within the data distorts retrieval of the mechanism more than uncertainty within the location and velocity modeling, (3) determination of the orientation of the mechanism is fairly robust with respect to all of the factors listed, excluding very poor station distributions. Retrieval of the DC versus non-DC content is more sensitive than the orientation. Poor station distributions may cause a large bias and reliable determination is a challenge for the inverse modelling of seismic sources. The key feature of the task is the complexity versus simplicity of the model. A complex model obviously has the capacity to describe in-depth properties of the source. However, complex models need not be resolvable using a limited data set. By applying a constraint, the model exactly simulates source processes that are simpler and relevant to certain realistic features. In many cases, however, simplification does not matter. The benefit of the acceptance of the simpler model is enhanced robustness of the inverse task. Acceptance of the STC as a source mechanism model implies a reduction of the number of parameters from six to five.

4 Confidence Zones

To assess the reliability of the solution obtained, I evaluated the confidence zones of source model parameters or their combinations. Confidence zones are objects within the model space that specify the volume in which the solution of the inverse task is captured in an a priori specified probability if errors in the data are taken into account. In other words, confidence zones describe a distribution for model parameters that yield a good match to the data. The size and shape of confidence zones indicate the uncertainty of the determined parameters. Large confidence zones indicate a poor solution while small confidence zones indicate a good solution. Both reliability for determining geometry, the orientation of the mechanism, and its characteristics for the DC and non-DC content, must be estimated. To assess geometric reliability, I constructed confidence zones for the T, P, and N axes of the deviatoric portion of the MT solution and confidence zones for decomposition of the MT in order to determine the characteristics for both the DC and non-DC content. For the STC model, I evaluated the same simply by re-computing the MT that corresponded to a given STC and additionally computing the confidence zone for the slope angle. For the procedure, I scanned the model space within a regular grid and evaluated a match to the data and the posterior probability density (PPD) for grid points. I then integrated the PPD across a trial volume within the model space and looked for a patch in which the cumulative probability acquired certain values, say, 0.9, 0.95, and 0.99.

I considered the confidence zone of the model parameters, $\boldsymbol{m}$, using the probability content, p, to be a set of points, $\boldsymbol{m}$, satisfying the following:

$$\chi^2(\boldsymbol{m}) < \chi^2_{\boldsymbol{p}} \tag{3}$$

where $\chi^2(\boldsymbol{m})$ is the misfit function constructed from the residual least squares of data and synthetics, and the dispersion, χ^2_p, is determined from the following condition:

$$\frac{\int_{\chi^2(\mathbf{m})<\$^2_{\mathbf{p}}} \mathrm{PPD}\ \mathrm{d}\mathbf{m}}{\int_{\mathbf{m}} \mathrm{PPD}\ \mathrm{d}\mathbf{m}} = \mathrm{p} \tag{4}$$

that specifies the ratio of the cumulative probability within the region to the integral of the posterior probability density (PPD; e.g., Tarantola 1987) across the entire model space. The PPD is defined as follows:

$$\mathrm{PPD} = \exp\left(-\frac{1}{2}\chi^2\right). \tag{5}$$

Schematically, it can be depicted by the cartoon in Fig. 5.

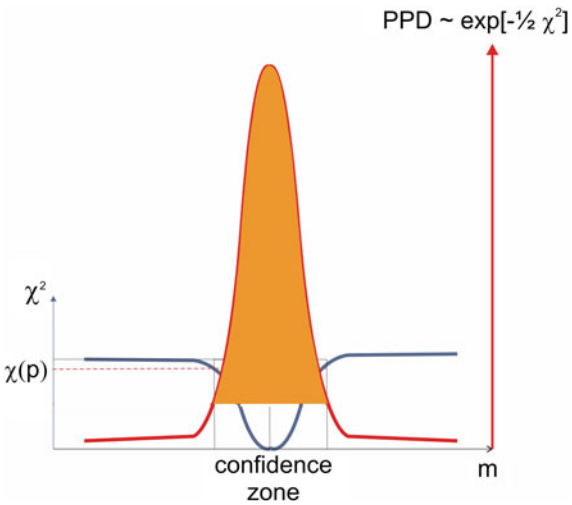

Fig. 5 A cartoon illustrating construction of a 1-D confidence interval. χ^2 is the residual function that is minimized during the course of the inversion, PPD is the posterior probability density function according to (5), and χ_p is the value satisfying (4)

Using the function $\chi^2(\boldsymbol{m})$, I determined particular confidence zones as regions limited by the contour χ^2_p that possessed the probability content requested (Šílený 1998). In particular, I constructed confidence zones for the P, T, and N axes of the DC portion of the mechanism that provided information on the uncertainty for determining orientation and the confidence zone for the slope angle that yielded information on the uncertainty of the shear versus non-shear content. High content for a non-shear slip component was indicated by increased uncertainty in the P and N axes in cases of a fault opening, and the T and N axes if the fault closed. For a pure tensile crack (mode I of the fracturing), the P and N (or T, N) axes were undetermined and their confidence zones were merged into a single belt within the plane perpendicular to the crack opening (or closing). For the case of the MT source model, I again investigated the confidence zones of the P, T, and N axes, as well as the MT decomposition in terms of the percentage of the double-couple (DC), the isotropic component (ISO), and the compensated linear vector dipole (CLVD).

5 Case Studies

5.1 Tectonic Earthquakes: West Bohemia

Advantageous robustness of the STC as compared to the MT can be demonstrated by verifying non-shear content within the mechanism of the W-Bohemia/Vogtland earthquake swarm from 1997 (Dahm et al. 2000). The W-Bohemia/Vogtland is an intraplate area with extinct Quaternary Period volcanism that manifests present geo-

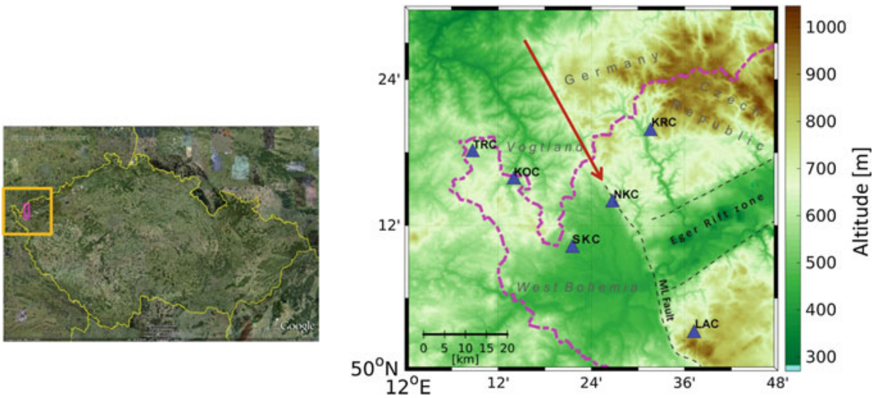

Fig. 6 The seismoactive area of west Bohemia/Vogtland. The figure on the right is a zoom-in of the yellow framed section within the Czech Republic (shown in the left figure) and displays stations (blue triangles) within the WEBNET seismic network that were active during 1997, as well as the principle tectonic features of the Mariánské Lázně (ML) Fault and the Eger Rift Zone (dashed black lines). The red arrow in the right figure marks the position of Nový Kostel, the most active portion of the zone. The purple line indicates the border between the Czech Rep. and Germany

dynamic unrest by persistent swarm seismicity and the degassing of a large amount of CO_2 of upper-mantle origin, Fig. 6. The local magnitudes of swarm events are most often lower than 4.0; larger earthquakes are rather exceptional.

During the 1997 swarm, two types of prevailing mechanisms were observed, one characterized by a notable non-DC component. Dahm et al. (2000) reviewed whether or not these mechanisms were real by changing the attenuation model during inversion and by changing the inversion approach. These authors inverted each single event into the MT, and also determined relative MTs for the entire group. The result was stability of the solutions and, thus, the non-DC component was declared to be reliable. By employing a constrained source model possessing the ability to resolve a volume change and by exhibiting better resolution than inversion into the full MT, the test conducted with the STC represents a good opportunity for checking this conclusion on a different basis. The conclusion has been confirmed by performing

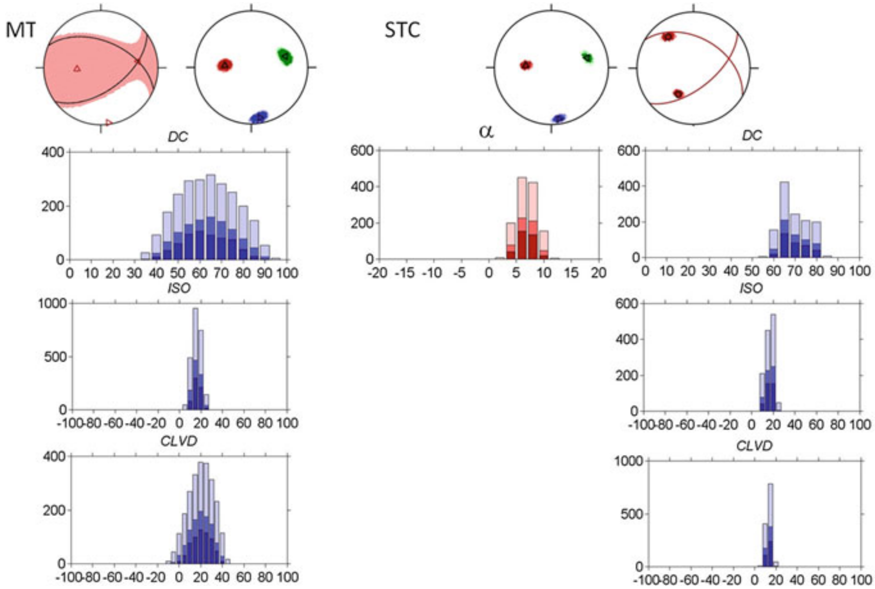

Fig. 7 Mechanism for the earthquake on January 26, 1997, 12:31:27, at a depth 9.2 km, M_0 1.95 $\times$ 10^{12} Nm, ML = 1.1 in relation to the MT (left) and the STC (right) source models. The MT portion is shown as follows: Top left, the fault-plane solution (solid lines are the nodal lines of the DC; triangle up, T-axis; triangle right, P-axis; triangle left, N-axis; and red patch, zone of P compressions) in an equal-area projection of the lower focal hemisphere. Top right, the T, P, and N axes and their confidence regions at the 90% (dark color), 95% (medium), and 99% (pale color) probability levels. From middle to bottom, the histograms, in turn, for the DC, ISO, and CLVD components displaying confidence regions for the 90% (dark color), 95% (medium), and 99% (pale color) probability levels. The STC: Top left, T, P, and N axes and their confidence regions at the 90, 95, and 99% probability levels. Top right, source lines (red) and the confidence regions of the poles for the source planes. Middle left, a histogram of the slope angle, α. Right from middle to bottom, histograms, in turn, for the DC, ISO, and CLVD components

the parallel MT and STC inversion using a confidence region estimate for events previously marked as non-DC phenomena. However, for several events, the non-DC component was determined to not be significant in terms of the confidence region evaluation. Here, I present an example of the former group (Fig. 7), whereas the non-DC characteristics of the event have been confirmed both by the MT and by the STC inversion (the ISO and CLVD histograms are out of the zero value for both the MT and STC solutions). However, thanks to markedly narrower confidence regions, the STC solution is preferred against the MT.

5.2 Earthquakes Induced by Fluid Injection into Geothermal Wells: Soultz-sous-Forêts, Alsace

The geothermal reservoir at Soultz-sous-Forêts is a unique natural laboratory for studying the mechanisms of micro-earthquakes generated during stimulations and circulation tests (Genter et al. 2009). Numerous hydraulic stimulation experiments have been performed in this area in recent decades with the aim of improving the connectivity of drilled boreholes within the natural fracture system. Stimulations were accompanied by abundant seismic activity, monitored by a surface network of 20+ stations with a very good azimuthal and distance distribution located near the site. Efforts regarding the retrieval of mechanisms occurring within this area were aimed at detecting the type of rock massif fracturing required to aid estimations of the permeability of the reservoir. Recent studies indicate a prevailingly shear slip. Rarely, a non-shear pattern has also been observed. As a default, a MT description has largely been applied. With the goal of assessing the resolution of the mechanism (both concerning orientation and, potentially, the non-DC content), Šílený et al. (2014) performed a series of synthetic experiments for testing the STC in comparison with the MT in the set-up of a seismic activity monitoring network. In addition to the complete configuration (23 stations surrounding the well-head) and four subsets mimicking deteriorating coverage, they assumed mismodeling of the velocity profile, hypocenter mislocation, and random noise contamination. The experiments exhibited clear dominance for the STC over the MT model, especially concerning DC/non-DC resolution. Then, the expectation of a better resolution was demonstrated on earthquakes from the reservoir (Fig. 8).

Here, there is obviously good similarity for the MT and STC solutions for monitoring geometry. Concerning orientation, both approaches yield practically the same results. However, as for the non-DC content, there is a difference. The STC solutions are closer to pure DCs and in several cases markedly closer (events 8, 12, 19, 23, and 25). Thus, in comparison to the MT, the STC behaves conservatively, reduces the non-DC suggested by the MT, and suggests that they may be spurious.

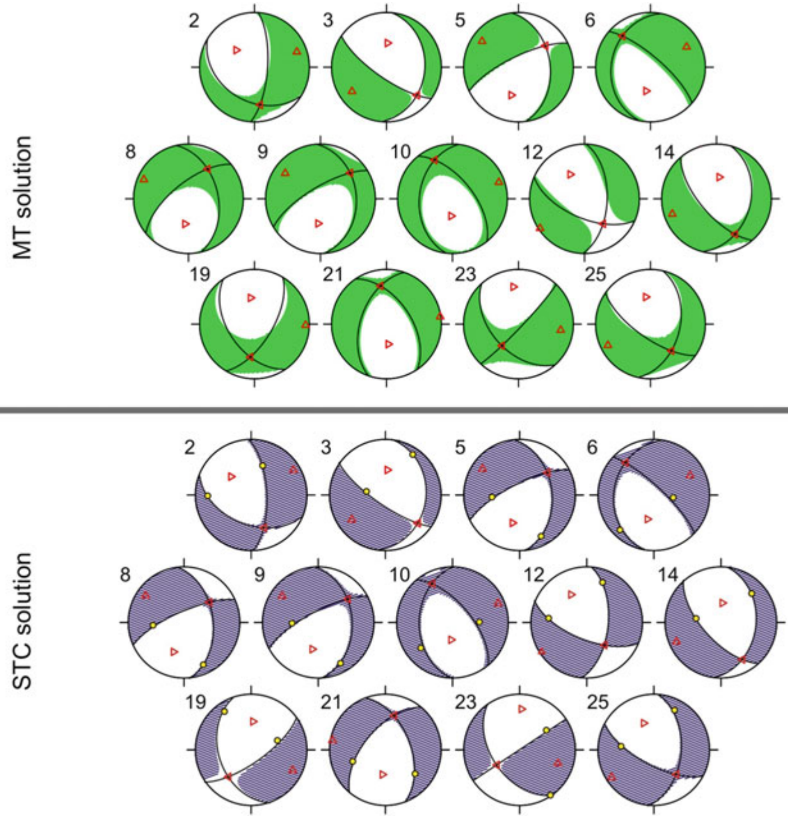

Fig. 8 A comparison of moment tensor (MT) solutions and shear-tensile crack (STC) solutions for 13 earthquakes occurring within the geothermal reservoir at Soultz-sous-Forêts. Source mechanisms are represented using traditional fault-plane solution plots. The nodal lines of the DC portion of retrieved MTs and source lines of the STC are shown as gray lines. The corresponding principal axes T, P, and N are shown with a triangle apex up, right, and left, respectively, within an equal-area, lower-hemisphere projection

5.3 Mining Associated Seismic Events Recorded at the Driefontein-Sibanye Gold Mine in South Africa

Dominance of the STC model over the traditional MT in resolving the mode of fracturing can be well-demonstrated in several mining-associated seismic events occurring at the Driefontein-Sibanye gold mine in South Africa. In the Introduction, I discussed the single-force and MT inversion of these events in relation to the Hasegawa models (Šílený and Milev 2008). In a follow-up paper, Šílený and Milev (2017) also determined their mechanisms based on the STC model, and complemented both inverse tasks by evaluating confidence regions in order to assess the uncertainty of solutions. The message of this upgrade for processing was twofold:

Table 1 A qualitative assessment of resolution for orientation of the mechanism and its decomposition using the MT and STC source models for five, mining-associated earthquakes recorded at the Driefontein-Sibanye Gold Mine in South Africa

Event			1	2	3	4	5
Resolution of orientation	MT	Single axis	Good	Fair	Fair	Excellent	Fair
		All 3 axes	Good	Poor	Poor	Poor	Very poor
	STC	Single axis	Excellent	Good	Good	Excellent	Fair
		All 3 axes	Excellent	Good	Good	Poor	Very poor
Resolution of decomposition: MT			Fair	Poor	Very poor	Very poor	Very poor
MT: DC versus non-DC			None	None	None	None	None
Resolution of decomposition: STC			Good	Good	fair	Fair	Excellent
STC: shear versus non-shear			**Implosion**	**Tensile**	**None**	**Tensile**	**Implosion**

(1) the orientation of the mechanism retrieved using the MT and STC is equal; and (2) the type of mechanism basically remains unchanged (i.e. relevance to the individual Hasegawa models mentioned above remains valid). The added value of upgraded processing (construction of the confidence regions), however, largely changed the view on the MT solution. Based on the results, it appeared that confidence of the DC versus non-DC assessment within the MT approach was very low, resulting in a non-DC percentage that could not be considered significant. Contrary to the MT, the STC offered a much more valuable outcome: the DC versus non-DC issue was resolved for all five events (Table 1) and allowed an interpretation of their mechanisms in terms of geomechanics.

5.4 Seismicity Due to the Hydrofracturing of Oil/Gas Wells: Cotton Valley, Texas

Hydrofracturing, the treatment aimed to enhance production, is routine within the oil and gas industry. Related seismicity provides valuable information on the success of the operation. Determination of the mechanisms yields information on the mode of rock-mass fracturing in terms of fracture mechanics: mode I (tensile crack) versus mode II (shear fracturing). Such knowledge is vital for mapping the permeability of the reservoir. Unfortunately, since observations are only performed from a few monitoring wells, the monitoring geometry is extremely unfavorable in this area. Even more problematic, the most frequent setup (monitoring within a single monitoring well) is a worst case scenario since an observation from only one azimuth is available. Then, far-field data are not sufficient for resolving the full MT (Nolen-Hoeksema

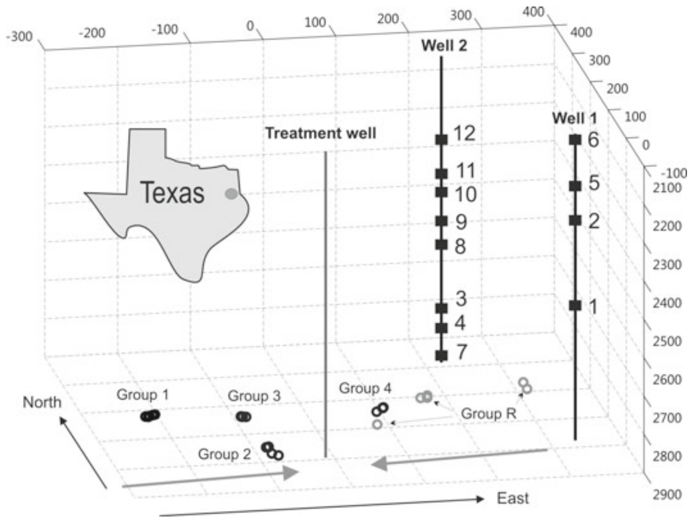

Fig. 9 An illustration of the hydraulic fracture imaging geometry for the Cotton Valley experiment (inset, gray dot on the sketch of Texas). Black heavy lines indicate monitoring wells 1 and 2 (full squares mark the positions of the geophones used in this study). The gray heavy line indicates the treatment well. The hypocenters of selected microearthquakes within groups G1–G4 and R are marked by circles. Gray arrows at the bottom of the model indicate the direction of maximum horizontal stress. Distance is provided in meters

and Ruff 2001; Vavryčuk 2007). The solution is adding more data (e.g., observations from a near-field (Song and Toksöz 2011), a priori constraints of the mechanism (Jechumtálová and Eisner 2008), or applying a constrained MT. Such a solution was performed by Grechka et al. (2016), who used the "tensile model", essentially the STC, and designed an inversion algorithm and demonstrated its performance on single-well data from the oil industry.

Here, I demonstrate improvement for the determination of a mechanism from data gathered within two monitoring wells. In theory, data from two wells is enough to obtain a full MT. Nevertheless, its resolution is still very poor due to extremely sparse coverage of the focal sphere. Thus, employment of a constrained MT is also reasonable here. As an example, I reinterpreted microearthquakes obtained from the Cotton Valley, E. Texas data set. The data were processed within the complete MT description by Šílený et al. (2009), in terms of the STC source model, and the MT and STC solutions were compared (Fig. 9).

Hydrofracturing of the treatment well resulted in abundant seismicity; classified by Rutledge et al. (2004) into several groups, G1-G4. Šílený et al. (2009) processed selected events from each group using a full MT analysis and determined notable non-DC mechanisms. However, some of the mechanisms seemed to be rather unrealistic, especially events from the G4 group. Šílený (2012) reprocessed them in terms of the STC source model and documented a similar fit for the data. The solutions were largely similar, in several cases (for the G4 group, especially) simpler mecha-

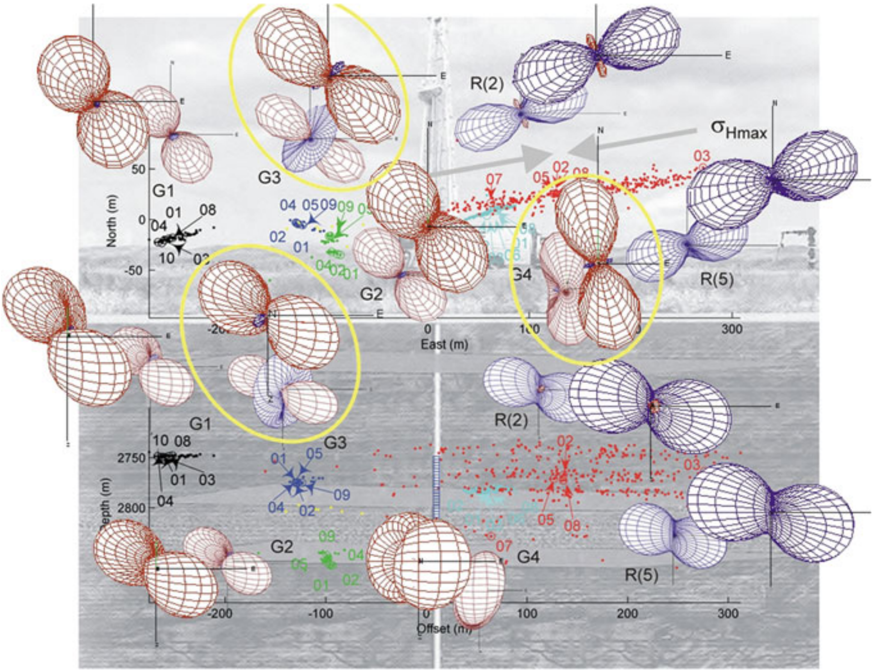

Fig. 10 Cotton Valley mechanisms for G1–G4 and R groups within the MT (smaller-size plots are provided in the background) and the STC (large-size plots are provided in the foreground) source description, plotted as 3-D, wire-frame diagrams of P radiation (red—expansion, blue—compression). The top panel provides a map view, while the bottom panel provides a depth section viewed from S. The MT solutions are reprinted from Šílený et al. (2009). MT versus STC couples that differed the most are provided in yellow ovals

nisms were obtained, allowing a more feasible interpretation from the viewpoint of geomechanics (Fig. 10).

6 Concluding Remarks

The moment tensor (MT) has become a standard for describing seismic sources, both in earthquake seismology and for various types of induced seismicity. In general, the MT is a dipole source but, in practice, may be too general because its generality causes trouble during its reconstruction from noisy data during the inverse process that may also be ill-conditioned due to an inexact hypocenter location and/or to the availability of a rough velocity/attenuation model. Then, the retrieved source may be biased. Thus, in practice, a constrained MT is frequently used. The traditional deviatoric constraint, routinely employed within Centroid Moment Tensor (CMT) solutions of moderate to strong earthquakes, may not be adequate for earthquakes without a purely tectonic origin (e.g., for volcanic earthquakes), among them events induced by industrial activities such as mining or fluid injection into boreholes. Therefore, it seems reasonable to use a simpler source model for directly describing the physical phenomena anticipated within a particular focus. The simple combination of a shear slip with a tensile crack or a 1D implosion (a Shear-Tensile Crack, STC) may be a good model both for natural earthquakes and induced events. In many cases, constraining the full MT helps one obtain a better resolution for the mechanism: sometimes the determination of its orientation and, very frequently, its double-couple (DC) versus non-DC content. Urgency for constraining the full MT increases with deteriorating quality of the geometry of the observation. With dense observations, well-distributed surrounding a focus, the full MT can yield good resolution for both the geometry and the non-DC content. Resolution especially falls due to notable gaps in station distribution. In extreme cases of sensor configuration depletion, during single azimuth monitoring, the MT completely fails and model simplification in terms of the STC is crucial.

Acknowledgements This work was supported by the following grant from the Czech Science Foundation: "Solid body fracturing mode by shear-tensile source model: acoustic emission laboratory study", Grant Agreement No. P108 16-03950S.

References

Aki K, Richards PG (2002) Quantitative seismology. Freeman, San Francisco

Braunmiller J, Kradolfer U, Baer M, Giardini D (2002) Regional moment tensor determination in the European–Mediterranean area—initial results. Tectonophysics 356:5–22

Dahm T, Horálek J, Šílený J (2000) Comparison of absolute and relative moment tensor solutions for the January 1997 West Bohemia earthquake swarm. Studia Geophys et Geodaet 44:233–250

Dreger DS, Helmberger DV (1993) Determination of source parameters at regional distances with three-component sparse network data. J Geophys Res 98:8107–8125

Dufumier H, Rivera L (1997) On the resolution of the isotropic component in moment tensor inversion. Geophys J Int 131:595–606. https://doi.org/10.1111/j.1365-246X.1997.tb06601.x

Dziewonski AM, Chou TA, Woodhouse JH (1981) Determination of earthquake source parameters from waveform data for studies of global and regional seismicity. J Geophys Res 86:2825–2852

Ekstrom G, Nettles M, Dziewonski AM (2012) Centroid-moment tensors for 13,017 earthquakes. Phys Earth Planet Int 200:1–9

Genter A, Fritsch D, Cuénot N, Baumgärtner J, Graff JJ (2009) Overview of the current activities of the European EGS Soultz project: from exploration to electricity production. In: Proceedings thirty-fourth workshop on geothermal reservoir engineering, Stanford, California, 9–11 Feb 2009, SGP-TR-187

Grechka V, Li Z, Howell B, Vavryčuk V (2016) Single-well moment tensor inversion of tensile microseismic events. Geophysics 208:1724–1739

Hasegawa HS, Wetmiller RJ, Gendzwill DJ (1989) Induced seismicity in mines in Canada—an overview. Pure Appl Geophys 129:423–453

Henry C, Woodhouse JH, Das S (2002) Stability of earthquake moment tensor inversions: effect of the double-couple constraint. Tectonophysics 356:115–124

Horálek J, Fischer T (2008) Role of crustal fluids in triggering the west Bohemia/Vogtland earthquake swarms: just what we know (a review). Stud Geophys Geodet 52:455–478

Jakobsdóttir SS, Roberts MJ, Gudmundsson GB, Geirsson H, Slunga R (2008) Earthquake swarms at Upptyppingar, north-east Iceland: a sign of magma intrusion? Stud Geophys Geodet 52:513–528
Jechumtálová Z, Eisner L (2008) Seismic source mechanism inversion from a linear array of receivers reveals non-double-couple seismic events induced by hydraulic fracturing in sedimentary formation. Tectonophysics 460:124–133. https://doi.org/10.1016/j.tecto.2008.07.011
Julian BR, Miller AD, Foulger GR (1998) Non-double-couple earthquakes 1. Theory. Rev Geophys 36:525–549
Kawakatsu H (1995) Automated near-realtime CMT inversion. Geophys Res Lett 22:2569–2572
Kubo A, Fukuyama E, Kawai H, Nonomura K (2002) NIED seismic moment tensor catalog for regional earthquakes around Japan: quality test and application. Tectonophysics 356:23–48
Malovichko DA (2005) Personal communication
Minson SE, Dreger DS, Bürgmann R, Kanamori H, Larson KM (2007) Seismically and geodetically determined nondouble-couple source mechanisms from the 2000 Miyakejima volcanic earthquake swarm. J Geophys Res 112:B10308. https://doi.org/10.1029/2006JB004847
Nolen-Hoeksema RC, Ruff LJ (2001) Moment tensor inversion of microseisms from the B-sand propped hydrofracture, M-site, Colorado. Tectonophysics 336:163–181
Nábělek J, Xia G (1995) Moment-tensor analysis using regional data: application to the 25 March, 1993, Scotts Mills, Oregon, earthquake. Geophys Res Lett 22:13–16
Okada Y (1985) Surface deformation due to shear and tensile faults in a half-space. Bull Seismol Soc Am 75(4):1135–1154
Pesicek JD, Šílený J, Prejean SG, Thurber CH (2012) Determination and uncertainty of moment tensors for microearthquakes at Okmok Caldera, Alaska. Geophys J Int 190:1689–1709. https://doi.org/10.1111/j.1365-246X.2012.05574.x
Pondrelli S, Morelli A, Ekström G, Mazza S, Boschi E, Dziewonski AM (2002) European-Mediterranean regional centroid-moment tensors: 1997–2000. Phys Earth Planet Int 130:71–101
Ritsema J, Lay T (1993) Rapid source mechanism determination of large (Mw $\geq$ 4.5) earthquakes in western United States. Geophys Res Lett 20:1611–1614
Rudajev V, Šílený J (1985) Seismic events with non-shear component II. Rock bursts with implosive source component. Pure Appl Geophys 123:17–25
Rutledge JT, Phillips WS, Mayerhofer MJ (2004) Faulting induced by forced injection and fluid flow forced by faulting: an interpretation of hydraulic-fracture microseismicity, Carthage Cotton Valley Gas Field. Bull Seism Soc Am 94:1817–1830
Stierle E, Vavryčuk V, Šílený J, Bohnhoff M (2014) Resolution of non-double-couple components in the seismic moment tensor using regional networks—I: a synthetic case study. Geophys J Int 196(3):1869–1877. https://doi.org/10.1093/gji/ggt502
Šílený J (1989) The mechanism of small mining tremors from amplitude inversion. PAGEOPH 129:309–324
Šílený J (2009) Resolution of non-double-couple-mechanisms: simulation of hypocenter mislocation and velocity structure mismodeling. Bull Seismol Soc Am 99. https://doi.org/10.1785/0120080335
Šílený J (2012) Shear-tensile/implosion source model vs. moment tensor: benefit in single-azimuth monitoring. Cotton Valley set-up. In: 74th EAGE conference & exhibition incorporating SPE EUROPEC 2012. Houten, EAGE, 2012, pp 1–5. ISBN 978-90-73834-27-9
Šílený J, Hill DP, Eisner L, Cornet FH (2009) Non–double-couple mechanisms of icroearthquakes induced by hydraulic fracturing. J Geophys Res 114:B08307. https://doi.org/10.1029/2008JB005987
Šílený J, Milev A (2008) Source mechanism of mining induced seismic events—resolution of double couple and non double couple models. Tectonophysics 456:3–15. https://doi.org/10.1016/j.tecto.2006.09.021
Šílený J, Milev A (2017) Mechanism of mining associated seismic events recorded at Driefontein-Sibanye gold mine in South Africa. In: Feng X-T (eds) Rock mechanics and engineering, vol 5, © CRC Press/Balkema, Taylor & Francis Group

Šílený J, Jechumtálová Z, Dorbath C (2014) Small scale earthquake mechanisms induced by fluid injection at the enhanced geothermal system reservoir Soultz (Alsace) in 2003 using alternative source models. Pure Appl Geophys 171:2783–2804. https://doi.org/10.1007/s00024-013-0750-2

Šílený J, Panza GF, Campus P (1992) Waveform inversion for point source moment tensor retrieval with variable hypocentral depth and structural model. Geophys J Int 109:259–274

Sipkin SA (1982) Estimation of earthquake source parameters by the inversion of waveform data: synthetic waveforms. Phys Earth Planet Int 30:242–259

Sipkin SA, Zirbes MD (2004) Moment-tensor solutions estimated using optimal filter theory: global seismicity, 2002. Phys Earth Planet Int 145:203–217

Song F, Toksöz MN (2011) Full-waveform based complete moment tensor inversion and source parameter estimation from downhole microseismic data for hydrofracture monitoring. Geophysics 76(6):WC103–WC116

Stich D, Ammon CJ, Morales J (2003) Moment tensor solutions for small and moderate earthquakes in the Ibero-Maghreb region. J Geophys Res 108, Art. No. 2148

Tarantola A (1987) Inverse problem theory. methods for data fitting and model parameter estimation. Elsevier, Amsterdam

Teisseyre R (1980) Some remarks on the source mechanism of rockhursts in mines and on the possible source extension. Acta Mont CSAV Praha 58:7–13

Vavryčuk V (2001) Inversion for parameters of tensile earthquakes. J Geophys Res 106:16339–16355. https://doi.org/10.1029/2001JB000372

Vavryčuk V (2007) On the retrieval of moment tensors from borehole data. Geophys Prospect 55(3):381–391

Vavryčuk V (2011) Tensile earthquakes: theory, modeling and inversion. J Geophys Res 116:B12320. https://doi.org/10.1029/2011JB008770

Vavryčuk V, Kim SG (2014) Nonisotropic radiation of the 2013 North Korean nuclear explosion. Geophys Res Lett 41:7048–7056. https://doi.org/10.1002/2014GL061265